PET Quantification of 5-HT_{2A} Receptors in the Human Brain: A Constant Infusion Paradigm with [^{18}F]Altanserin

Christopher H. van Dyck, Ping-Zhong Tan, Ronald M. Baldwin, Louis A. Amici, Pradeep K. Garg, Chin K. Ng, Robert Soufer, Dennis S. Charney, and Robert B. Innis

Departments of Psychiatry and Diagnostic Radiology, Yale University School of Medicine, New Haven; and West Haven Veterans' Affairs Medical Center, West Haven, Connecticut

[^{18}F]altanserin has been used to label serotonin 5-HT_{2A} receptors, which are believed to be important in the pathophysiology of schizophrenia and depression. The purpose of this study was to test the feasibility of a constant infusion paradigm for equilibrium modeling of [^{18}F]altanserin with PET. Kinetic modeling with [^{18}F]altanserin may be hampered by the presence of lipophilic radiometabolites observed in plasma after intravenous administration. **Methods:** Eight healthy volunteers were injected with [^{18}F]altanserin as a bolus (208 ± 9 MBq [5.62 ± 0.25 mCi]) plus constant infusion (65 ± 3 MBq/h [1.76 ± 0.08 mCi/h]) ranging from 555 to 626 min (615 ± 24 min) after injection. PET acquisitions (10–20 min) and venous blood sampling were performed every 30–60 min throughout the infusion period. **Results:** Linear regression analysis revealed that time–activity curves for both brain activity and plasma [^{18}F]altanserin and metabolite concentrations stabilized after about 6 h. This permitted equilibrium modeling and estimation of V_3' (ratio of specific uptake [cortical–cerebellar] to total plasma parent concentration after 6 h). Values of V_3' ranged from 1.57 ± 0.38 for anterior cingulate cortex to 1.02 ± 0.39 for frontal cortex. The binding potential V_3 (ratio of specific uptake to free plasma parent concentration after 6 h, using group mean f_1) was also calculated and ranged from 169 ± 41 for anterior cingulate cortex to 110 ± 42 for frontal cortex. From 6 h onward, the rate of change for V_3' and V_3 was only 1.11 ± 1.69 %/h. **Conclusion:** These results demonstrate the feasibility of equilibrium imaging with [^{18}F]altanserin over more than 5 radioactive half-lives and suggest a method to overcome difficulties associated with lipophilic radiolabeled metabolites. The stability in V_3 and V_3' once equilibrium is achieved suggests that a single PET acquisition obtained at 6 h may provide a reasonable measure of 5-HT_{2A} receptor density.

Key Words: [^{18}F]altanserin; 5-HT_{2A} receptor; serotonin; PET

J Nucl Med 2000; 41:234–241

In vitro studies on human brain autopsy material have revealed alterations in serotonin 5-HT_{2A} receptors in a variety of conditions, including depression/suicide (*1,2*), schizophrenia (*3,4*), aging (*5*), and Alzheimer's disease (*6,7*). Recently, the use of PET has allowed in vivo imaging of the regional brain distribution of 5-HT_{2A} receptors (*8*). However, PET radioligands for 5-HT_{2A} receptor imaging, such as ^{11}C-3-*N*-methyl-spiperone (NMSP) (*9*) and [^{18}F]-setoperone (*10*), lack specificity, binding with moderate to high affinity to dopamine D_2 receptors. As a result, considerable effort has been directed to the development of more selective 5-HT_{2A} ligands for PET (*11,12*).

[^{18}F]altanserin (*11,13*), a 4-fluorobenzoyl-piperidine derivative structurally related to ketanserin and setoperone, has emerged as a promising PET ligand for 5-HT_{2A} receptors. Compared with previous 5-HT_{2A} radiotracers, [^{18}F]altanserin yields higher ratios of specific-to-nonspecific binding and greater selectivity for 5-HT_{2A} receptors compared with other monoamine receptors (*14*). Altanserin has more than a 20-fold greater selectivity for 5-HT_{2A} than any other 5-HT receptor subtype, including the 5-HT_{2C}, which has significant homologies to 5-HT_{2A} (*15*). Kinetic modeling with [^{18}F]altanserin has previously been used in initial human studies (*16–19*), but may be hampered by the presence of nonspecifically bound lipophilic radiometabolites observed in plasma after intravenous administration (*15,20,21*), resulting in the need to identify a large number of rate constants.

The purpose of this study was to test the feasibility of a constant infusion paradigm for equilibrium modeling of [^{18}F]altanserin with PET. Because of problems associated with kinetic analysis of single bolus experiments, we implemented an alternative paradigm based on constant infusion of the radiotracer. This paradigm creates and maintains a prolonged state of equilibrium at the level of the receptors, allowing direct measurement of the distribution volumes of the tracer (*22,23*). The presence of lipophilic radiometabolites poses a challenge for an equilibrium approach as well, but the modeling is considerably simpler. That is, if the metabolites are inactive (*15,21*) and distribute uniformly in brain, then subtraction of background from a target region at the time of equilibrium provides specific receptor binding, corrected for the presence of metabolites. Other advantages of an equilibrium approach include the absence of arterial plasma sampling and the relatively short

Received Jul. 27, 1998; revision accepted Jul. 30, 1999.

For correspondence or reprints contact: Christopher H. van Dyck, MD, Yale University School of Medicine, CB 2041, 333 Cedar St., New Haven, CT 06510.

imaging time (20–40 min), once the methodology has been validated for clinical studies.

MATERIALS AND METHODS

Radiopharmaceutical Preparation and Purity

[^{18}F]altanserin was synthesized in a complete remote control system (*24*) modified from a method previously described (*11*). The precursor nitro-altanserin, 3-(2-(4-(4-nitrobenzoyl)-1-piperidinyl)-ethyl)-1,2-dihydro-2-thioxo-4-quinazolinone, was prepared from commercial reagents with >99.0% purity (*25*). For these 8 PET studies, 2057 ± 322 MBq (55.6 ± 8.7 mCi; with these and subsequent data expressed as mean ± SD, unless otherwise specified; SEM is used in Figs. 1, 2, and 4 for legibility) [^{18}F]altanserin were produced, with an overall radiochemical yield of 10.3% ± 2.5% at the end of synthesis. Radiochemical purity was 99.0% ± 1.3% and specific activity 46,546 ± 18,981 MBq/μmol (1258 ± 513 mCi/μmol) (range, 22,533–75,591 MBq/μmol [609–2043 mCi/μmol]) at the time of injection and start of infusion, as determined by high-performance liquid chromatography (HPLC) (EM RP Select-B [EM Science, Gibbstown, NJ]; 250 × 4.6 mm, 10 μm, tetrahydrofuran-to-sodium acetate buffer, 35:65 [pH 5.0] at 2.5 mL/min). The synthesis time was 112 ± 9 min (range, 97–124 min). The total mass dose of [^{18}F]altanserin administered during the bolus plus constant infusion study was 0.14 ± 0.05 μg/kg (range, 0.10–0.24 μg/kg). Sterility was confirmed by lack of growth in 2 media: fluid thioglycollate and soybean-casein digest (*26*). Apyrogenicity was confirmed by the LAL test (Endosafe, Charleston, SC).

Study Population

The study population included 8 healthy volunteers (3 men, 5 women; age range, 25–42 y; mean age, 32.1 ± 5.6 y) and ranged in weight from 43 to 82 kg (63.8 ± 12.5 kg). Volunteers underwent clinical examinations by a research psychiatrist to exclude any neurological or psychiatric disease or alcohol or substance abuse. Screening procedures included a physical and neurological examination, electrocardiography, serum chemistries, thyroid function studies, complete blood cell count, urinalysis, and urine toxicology screen. In addition, each volunteer underwent brain MRI that was read as normal by a neuroradiologist. No volunteer, according to self-report, had taken centrally active medication within 1 mo of PET scanning. All volunteers gave written informed consent to the research protocol approved by the local human investigation committee.

PET Data Acquisition

Based on preliminary studies in 5 healthy volunteers (data not shown), a bolus/infusion (hourly infusion rate) ratio of 3.2 was selected for the present analysis. [^{18}F]altanserin (208 ± 9 MBq [5.62 ± 0.25 mCi]) was injected intravenously (through the constant infusion line) as a single bolus over 30 s at approximately 12 noon, and a constant infusion of 65 ± 3 MBq/h (1.76 ± 0.08 mCi/h) was started and ran in duration from 555 to 626 min (615 ± 24 min). Thus, the total administered dose (incorporating decay of the isotope) was 377 ± 19 MBq (10.2 ± 0.5 mCi). The actual bolus/infusion ratio for the 8 volunteers was 3.20 ± 0.02.

Volunteers were placed in the Posicam 6.5 camera (Positron Corp., Houston, TX) at the Yale/Veterans' Affairs PET Center, with head positioned by laser along the canthomeatal line and immobilized with straps. Repositioning after periods out of the scanner was accomplished by realigning the laser lights with marks placed along the canthomeatal line and glabella. The Posicam 6.5 is a 21-slice camera with 5.125-mm interslice distance. The resolution of the camera is 5.8 mm in-plane and 11.9 mm in the z axis. In-plane resolution after filtering with the Butterworth filter is 7.5 mm. The sensitivity of the camera measured in a 20-cm-diameter cylinder phantom is 165 kcts/s/μCi/mL (*27*). Five fiducial markers filled with 0.5–1.0 μCi ^{18}F were attached to the skin along the canthomeatal plane to identify this plane during image analysis. PET was performed throughout the [^{18}F]altanserin infusion period according to the following protocol: 10-min frame mode acquisitions starting at approximately 45, 90, 120, 180, 240, and 300 min after injection; then 20-min frame mode acquisitions starting at approximately 360, 390, 450, 480, 510, 540, 570, and 600 min after injection. PET and plasma data were more densely sampled from 6 h onward to evaluate the assumptions of the equilibrium model more reliably late in the study. To minimize repositioning errors, volunteers remained in the scanner for up to 3 h at a time, taking 2 breaks out of the scanner during the experiment.

PET Image Analysis

PET images were reconstructed using a deconvolution technique for scatter correction and a Butterworth filter (cutoff, 0.09/mm; power factor, 10) and displayed as a 256 × 256 matrix (pixel size, 1.7 × 1.7 mm; slice thickness, 5.125 mm; voxel volume, 14.81 mm^3). Attenuation correction was performed assuming uniform attenuation equal to that of water (attenuation coefficient, μ = 0.096/cm) within an ellipse drawn around the skull as identified by the markers. A cylindrical (20-cm diameter) fluid-filled phantom was scanned on the day of each study to obtain a calibration factor for each of the 21 slices for conversion of radioactivity into units of nCi/mL.

Region of interest (ROI) analysis was performed by an investigator using the Analyze7C image analysis program (CNSoftware, Wilmington, DE) running on a Sun SPARC station 20 (Sun Microsystems, Inc.; Mountain View, CA). ROI analysis was conducted for 6 cortical structures (frontal, anterior cingulate, orbitofrontal, temporal, parietal, and occipital cortices) and cerebellum. These regions were identified by comparison with a neuroanatomical atlas (*28*). ROIs were drawn on the PET image using a mouse-driven cursor. The ROI map was drawn individually for each volunteer with respect to the first PET acquisition and was applied uniformly to all subsequent acquisitions for that person. ROI analysis was performed in 17 of the 21 slices, with the inferior slice chosen to correspond best to the level of the fiducial markers (canthomeatal plane). The superior slice was thus centered approximately 8.7 cm above the canthomeatal plane.

A mean count density (cpm/pixel) was obtained for each anatomic structure in each acquisition by averaging values across all slices in which the structures appeared. Count densities were then decay-corrected for the time of injection and expressed in nCi/mL to generate brain time–activity curves.

Plasma Metabolite Analysis

An intravenous line was inserted in the arm opposite the constant infusion line for obtaining venous blood samples. Venous blood samples were obtained throughout the [^{18}F]altanserin infusion period at approximately 30, 60, 120, 180, 300, 360, 390, 420, 450, 480, 510, 540, 570, 600, and 630 min after injection.

Metabolite analysis was based on a published procedure (*16*). Plasma (2 mL) was diluted with 20 mL 50 mmol/L acetic acid and trapped on a C_{18} solid-phase extraction cartridge (Sep-Pak Lite; Waters Associates, Milford, MA) preconditioned with methanol

and water, washed with 10 mL 0.1% Et_3N followed by 5 mL H_2O, then eluted with 1 mL MeOH. The methanol eluate was diluted with an equal volume H_2O, and the entire solution was analyzed by HPLC on a Waters Novapak C_{18}, 3.9 × 300 mm column; mobile phase CH_3CN/0.353 mol/L HOAc/0.17 mol/L NH_4OAc (pH 4.9) (40:50:10), at a flow rate of 1.0 mL/min, with in-line ultraviolet detector (291 nm) and flow-through NaI scintillation detector/rate meter. Recovery of radioactivity using this procedure was 88.5% ± 6.0%, measured by adding tracer to blood and carrying out the same procedure. For identification of radiometabolites, the radioactive methanol/water solution was mixed with 3 authentic compounds (altanserin, altanserinol, and 4-(*p*-fluorobenzoyl)piperidine [FBP]) and injected on the HPLC.

Plasma protein binding was measured by ultrafiltration as previously described (*29*). The binding to plasma proteins was assumed to be rapid compared with the other processes measured in these experiments. As a consequence, the free fraction of plasma parent compound (f_1 = free parent/$C_p(t)$) (*30*) was assumed to be constant for all blood samples in a single experiment.

Equilibrium Model

Equilibrium analysis was performed using a 3-compartment model, comprising the plasma compartment (C_p); the intracerebral nondisplaceable compartment (C_2), in which the tracer can be free or nonspecifically bound; and the specifically bound compartment (C_3). At equilibrium, the venous concentration of tracer is assumed to approximate the arterial concentration and is taken as a measure of C_p. The equilibrium distribution volume of a compartment i (V_i) is defined as the equilibrium ratio of the tracer concentration in that compartment to the free plasma concentration: $V_i = C_i/(f_1C_p)$; where f_1 = free fraction of parent tracer in plasma. V_3 is equal to the binding potential (BP), which is the ratio of the receptor density (B_{max}) to the dissociation constant (K_D) (*30*).

The activity concentration in a receptor-rich cortical ROI at time t, $C_{ctx}(t)$, is the sum of the concentrations of the nondisplaceable [^{18}F]altanserin, the specifically bound [^{18}F]altanserin, and the radioactive metabolites (which are also assumed to be nondisplaceable):

$$C_{ctx}(t) = C_2(t) + C_3(t) + C_{met}(t).$$

Cerebellum has a relatively low concentration of 5-HT_{2A} receptors (*31–33*). If cerebellum is assumed to be devoid of 5-HT_{2A} receptors, then the activity concentration there at time t, $C_{cbl}(t)$, is the sum of the concentrations of the nondisplaceable [^{18}F]altanserin and the radioactive metabolites:

$$C_{cbl}(t) = C_2(t) + C_{met}(t).$$

If C_2 and C_{met} are further assumed to be uniform throughout the brain, then the specific binding in any receptor-rich cortical region may be estimated as:

$$C_3(t) = C_{ctx}(t) - C_{cbl}(t).$$

The equilibrium volume of distribution of compartment i is the ratio of the tracer concentration in compartment i to the free tracer concentration in the plasma at equilibrium, i.e., when no net transfer between the plasma and compartment i exists:

$$V_i = C_i/F_1C_p.$$

V_i' is defined as the ratio of the tracer concentration in compartment i to the total tracer concentration in the plasma at equilibrium:

$$V_i' = C_i/C_p.$$

At equilibrium, 2 different outcome measures can be derived. V_3, the equilibrium volume of distribution of the specifically bound compartment, is an estimate of the BP and is calculated as the ratio of the specific to the plasma free parent concentration:

$$V_3 = BP = C_3/f_1C_p.$$

At tracer radioligand concentration, BP equals B_{max}/K_D, in which B_{max} is the density of sites and K_D is the equilibrium dissociation constant (*34*). V_3' is a similar ratio to the total parent (which therefore does not depend on f_1—only about 1% for altanserin):

$$V_3' = C_3/C_p.$$

Statistical Analysis

The proposed equilibrium model relies on several assumptions, the most important of which is the stability over time of specific tracer uptake and free plasma parent concentrations. Average time–activity curves for both PET and plasma measurements were generated and visually examined to determine when a state of sustained equilibrium appeared to be achieved. To measure the stability of PET and plasma parameters from this time onward, the hourly rate of change for each parameter was computed by dividing the linear regression slope by the mean value of the parameter.

The equilibrium model was then applied to the entire sample to calculate the distribution volumes V_3 (C_3/f_1C_p) and V_3' (C_3/C_p). The effect of age on V_3 and V_3' was examined by Pearson's product moment correlation coefficient (r). Finally, the stability of the distribution volumes V_3 and V_3' at equilibrium was assessed by computing the hourly rate of change of the distribution volumes for each volunteer and for the entire sample.

RESULTS

None of the volunteers experienced any subjective or objective reactions. All vital signs (pulse, blood pressure, and respirations) were recorded before and 15–60 min after bolus injection and start of constant infusion, and serum chemistry profile, complete blood count, and urinalysis were repeated the day after the [^{18}F]altanserin PET study. No clinically significant effects on vital signs or laboratory studies were observed.

Seven of 8 volunteers completed planned [^{18}F]altanserin infusions of at least 620 min. Because of a technical problem, 1 volunteer completed an infusion of only 555 min; her data were not used to determine stability of regional brain uptake and plasma parent activity but were included in the final computations of V_3 and V_3'. Inspection of average plasma metabolite concentrations (Fig. 1A) and average PET time–activity curves (Fig. 2) suggested that equilibrium was attained after approximately 6 h of [^{18}F]altanserin infusion. To examine the stability of plasma and brain parameters after 6 h, the hourly rate of change for each parameter was computed by dividing the linear regression slope by the average value of the parameter from 6 to 10.5 h for the 7 volunteers who completed the full infusion experiment.

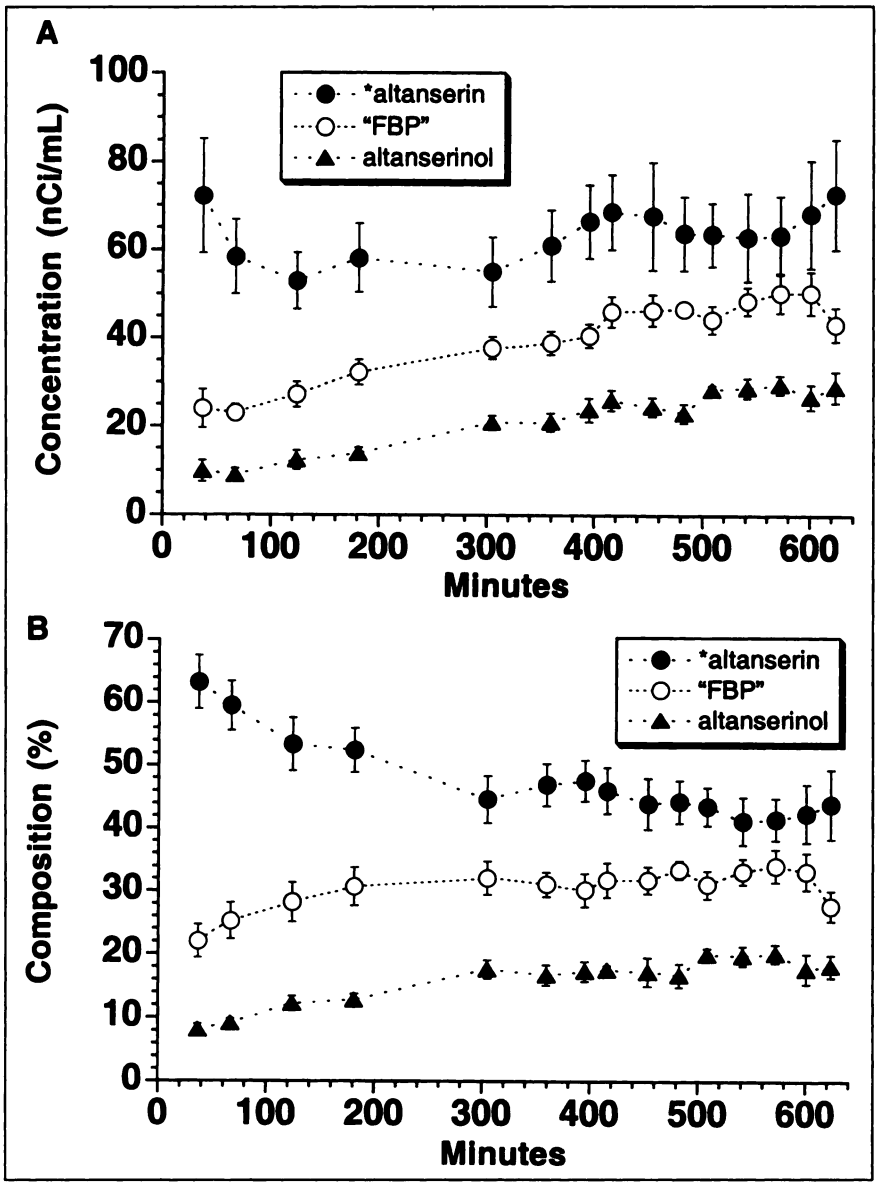

FIGURE 1. Average plasma metabolite concentrations (A) and percentage composition (B) (mean ± SEM used for legibility) after [^{18}F]altanserin infusion in 7 volunteers studied for at least 620 min. (One volunteer whose infusion duration was 555 min is not included.) Two missing plasma samples (out of 105 total) were handled by using linear interpolation of preceding and subsequent samples for that subject. From 6 h onward, rates of change were low for altanserin (−0.69 ± 5.21 %/h) and major lipophilic metabolite fraction ("FBP"; 3.64 ± 1.90 %/h), whereas some increase was still observed in minor lipophilic metabolite altanserinol (5.78 ± 9.02 %/h). Percentage of unchanged [^{18}F]altanserin fell from 63% at 37 min after injection and stabilized at approximately 45% from 6 h onward.

Plasma Metabolite Concentrations After [^{18}F]Altanserin Infusion

Three major plasma components were observed in these experiments. [^{18}F]altanserin parent (HPLC retention time t_R, 10.7 ± 0.3 min) and the ketone reduction product [^{18}F]altanserinol (t_R, 8.1 ± 0.2 min) were identified by comparison to authentic standards co-injected with the radioactive plasma samples. The third metabolite fraction had retention time (t_R, 6.2 ± 0.1 min) close but not identical to that of authentic FBP (t_R, 5.6 ± 0.1 min), the product of N-dealkylation on the piperidine ring. Results from other studies (*15,20,21*) suggest that this fraction actually consists of a mixture of metabolites, some of which may be secondary metabolites of FBP. In the present analysis, these additional metabolites are presumed to be contained in the FBP peak on HPLC and are included in the "FBP" time–activity curves.

Average plasma metabolite concentrations after [^{18}F]altanserin infusion in the 7 volunteers studied for at least 620 min are displayed in Figure 1A. The average time–activity curve for [^{18}F]altanserin appeared to level off by approximately 6 h after injection. From 6 h onward, mean rates of change were low for altanserin (0.69 ± 5.21 %/h) and the major lipophilic metabolite fraction ("FBP"; 3.64 ± 1.90 %/h), whereas some increase was still observed in the minor lipophilic metabolite altanserinol (5.78 ± 9.02 %/h).

The kinetics of unmetabolized [^{18}F]altanserin and metabolites as a fraction of the plasma activity are shown in Figure 1B. The percentage of unchanged [^{18}F]altanserin fell from 63% at 37 min after injection and stabilized at approximately 45% from 6 h onward.

PET Time–Activity Curves After [^{18}F]Altanserin Infusion

Representative [^{18}F]altanserin PET images from early and late time points are displayed in Figure 3. [^{18}F]altanserin uptake is high and relatively uniform in all cerebral cortical

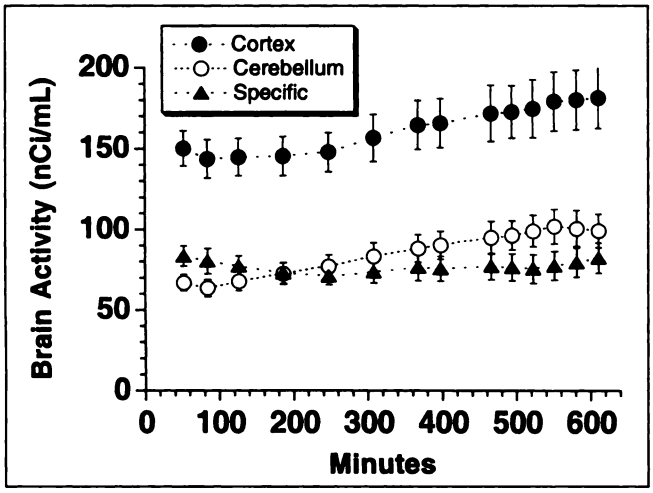

FIGURE 2. Average PET time–activity curves (mean ± SEM used for legibility) after [^{18}F]altanserin infusion in 7 volunteers studied for at least 620 min. (One volunteer whose infusion duration was 555 min is not included.) Three missing PET scans (out of 98 total) were handled using linear interpolation of preceding and subsequent samples for that subject. Cortex represents composite of all 6 cortical regions analyzed. From 6 h onward, rates of change were low for receptor-rich cortical regions (2.46 ± 1.03 %/h), receptor-poor cerebellum (3.45 ± 2.10 %/h), and specifically bound (cortex–cerebellum) tracer uptake (1.16 ± 2.00 %/h).

regions and low in basal ganglia, thalamus, and cerebellum.

Average PET time–activity curves after [^{18}F]altanserin infusion in the 7 volunteers studied for at least 620 min are displayed in Figure 2. From 6 h onward, rates of change were low for receptor-rich cortical regions (2.46 ± 1.03 %/h), receptor-poor cerebellum (3.45 ± 2.10 %/h), and specifically bound (cortex–cerebellum) tracer uptake (1.16 ± 2.00 %/h) (Table 1).

Equilibrium Outcome Measures

The outcome measures derived at equilibrium (averaging each volunteer's data from 6 to 10.5 h after injection) for cortical brain regions in all 8 volunteers are displayed in Table 2. Ratios of total-to-nonspecific (cerebellar) binding between 6 and 10.5 h after injection were 1.97 ± 0.16 for the structure of highest uptake (anterior cingulate) and 1.75 ± 0.15 for whole cortex. Values of V_3' (C_3/C_p) ranged from a high of 1.57 ± 0.38 for anterior cingulate cortex to 1.02 ± 0.39 for frontal cortex. Measurements of f_1 were used to calculate V_3 (C_3/f_1C_p) as an estimate of the BP. Values of f_1 ranged from 0.36% to 2.00% (0.93% ± 0.63%). V_3 was computed using both group mean and individual values of f_1.

Values of V_3' (and therefore V_3, using a mean f_1) were significantly correlated with age in this small sample for whole cortex ($r = -0.73$; $P < 0.05$) as well as orbitofrontal cortex ($r = -0.79$; $P < 0.05$), frontal cortex ($r = -0.79$; $P < 0.05$), anterior cingulate cortex ($r = -0.70$; $P < 0.05$),

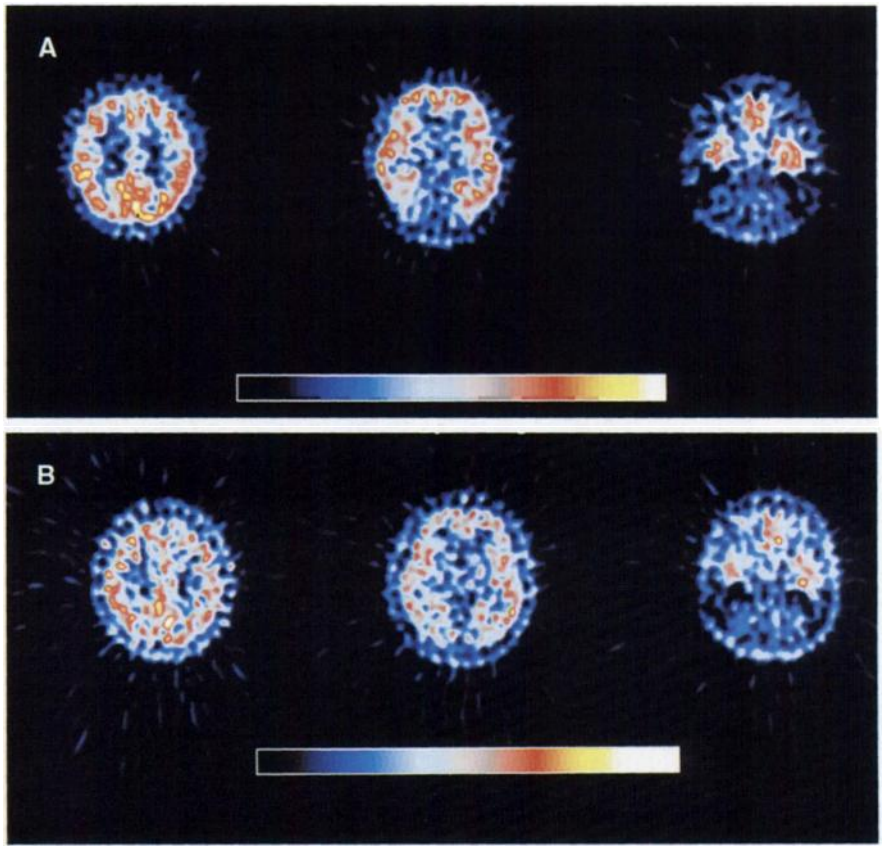

FIGURE 3. Transaxial PET images of [^{18}F]altanserin uptake in healthy volunteer at early and late time points: (A) 10-min acquisition starting 52 min after injection and (B) 40-min acquisition starting 376 min after injection. Uptake of [^{18}F]altanserin is consistent with known distribution of 5-HT_{2A} receptors as seen in autoradiographic studies, with high and relatively uniform uptake in all cerebral cortical regions, low uptake in basal ganglia and thalamus, and much lower uptake in cerebellum. Slices are situated approximately 80 (high cortex), 45 (thalamus and basal ganglia), and 10 mm (cerebellum) above canthomeatal plane. Later images are from single long acquisition obtained at equilibrium, as could be used in clinical study.

TABLE 1
Rates of Change in Plasma Metabolites and PET Brain ROIs at Equilibrium

Metabolites and ROIs	% Change/h* Mean	SD
Plasma metabolite		
Altanserin†	0.69	± 5.21
"FBP"	3.64	± 1.90
Altanserinol	5.78	± 9.02
Brain ROI		
Anterior cingulate cortex	3.33	± 1.13
Frontal cortex	1.38	± 1.84
Orbitofrontal cortex	2.70	± 3.11
Parietal cortex	2.78	± 1.22
Temporal cortex	2.50	± 1.30
Occipital cortex	2.67	± 1.61
Combined cortex	2.46	± 1.03
Cerebellum	3.45	± 2.10
Cortical specific binding	1.16	± 2.00

"FBP" = major lipophilic metabolite fraction, probably derived from 4-(*p*-fluoro-benzoyl)piperidine, as explained in text.

*Values are obtained by dividing the linear regression slope by mean value from 6 to 10.5 h after injection in 7 volunteers studied for at least 620 min.

†Parent compound.

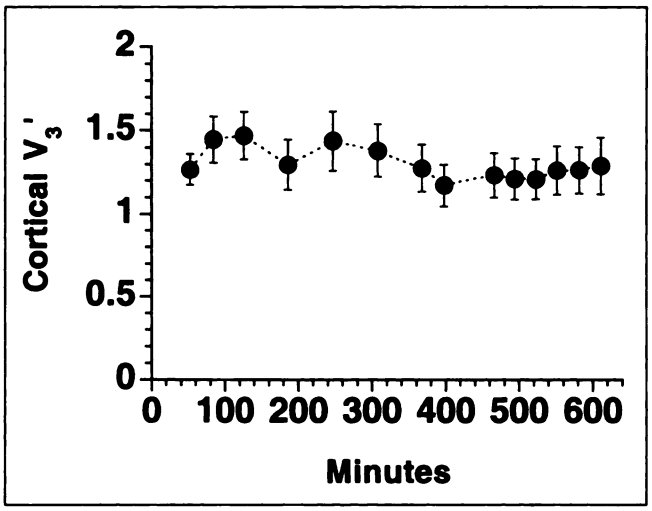

FIGURE 4. Stability of outcome measure V_3' for combined cortex (mean ± SEM used for legibility) after [^{18}F]altanserin infusion in 7 volunteers studied for at least 620 min. (One volunteer whose infusion duration was 555 min is not included.) For each PET acquisition of each volunteer, V_3' (ratio of specific uptake [cortical–cerebellar] to total plasma parent concentration) was derived using plasma sample nearest in time to midpoint of PET acquisition. From 6 h onward, mean rate of change was low for cortical V_3' (1.11 ± 1.69 %/h).

and parietal cortex ($r = -0.69$; $P < 0.05$). However, values for V_3 using individual f_1 values were uncorrelated with age. This age-related decline in 5-HT_{2A} receptors has been previously reported in both postmortem (*5*) and in vivo PET (*35–37*) studies.

Once equilibrium was achieved, values of V_3' (and therefore V_3, using mean or individual values of f_1) demonstrated excellent stability as shown in Figure 4 and Table 3. From 6 h onward, the rate of change for V_3' was 1.11 ± 1.69 %/h for the 7 volunteers studied for at least 620 min. Moreover, this rate of change did not exceed ±5%/h for any volunteer (Table 3).

TABLE 2
Outcome Measures at Equilibrium with [^{18}F]Altanserin in 8 Volunteers*

Cortex	Total/ cerebellar*	V_3'†	V_3 (mean f_1)‡	V_3 (indiv. f_1)§
Anterior cingulate	1.97 ± 0.16	1.57 ± 0.38	169 ± 41	248 ± 149
Frontal	1.63 ± 0.24	1.02 ± 0.39	110 ± 42	179 ± 130
Orbitofrontal	1.79 ± 0.15	1.28 ± 0.35	138 ± 37	204 ± 126
Parietal	1.88 ± 0.13	1.43 ± 0.34	153 ± 37	224 ± 135
Temporal	1.74 ± 0.18	1.20 ± 0.38	129 ± 41	187 ± 127
Occipital	1.70 ± 0.13	1.17 ± 0.41	126 ± 44	175 ± 102
Combined	1.75 ± 0.15	1.23 ± 0.32	132 ± 34	198 ± 128

*All values are obtained as the average of data between 6 and 10.5 h after injection.

†V_3' is calculated as ratio of specific (cortex–cerebellum) to the plasma total parent concentration (C_3/C_p). V_3 is calculated as ratio of specific to plasma free parent concentration (C_3/f_1C_p; equivalent to BP).

‡V_3 (mean f_1) uses group mean value of f_1 (0.93%).

§V_3 (indiv. f_1) uses individual values of f_1.

DISCUSSION

The major finding of this study is that [^{18}F]altanserin is a suitable radioligand for bolus plus constant infusion studies for equilibrium modeling with PET. Stable time–activity curves for both plasma and PET measurements suggest that a state of sustained equilibrium is achieved by approximately 6 h, permitting direct measurement of distribution volumes V_3 and V_3'. These results afford an alternative to kinetic modeling for quantification of 5-HT_{2A} receptors in the human brain using [^{18}F]altanserin and PET.

The proposed equilibrium model for [^{18}F]altanserin sug-

TABLE 3
Stability of V_3' at Equilibrium in Individual Volunteers

Volunteer no.	% Change/h*
1	3.08
2	2.79
3	−1.68
4	−0.21
5	1.83
6	1.41
7	0.59
Mean	1.11
SD	1.69

*Values are obtained by dividing linear regression slope by mean value from 6 to 10.5 h after injection.

gests a novel method to overcome difficulties associated with lipophilic radiolabeled metabolites. Whereas kinetic studies with [^{18}F]altanserin (*16–19*) have required complex modeling to identify a large number of rate constants, equilibrium modeling with [^{18}F]altanserin (assuming uniform uptake of nondisplaceable [^{18}F]altanserin and metabolites) permits the estimation of specific binding in a receptor-rich cortical region by simply subtracting cerebellar activity.

Plasma Measurements

The plasma analysis used in these experiments allowed quantitating parent [^{18}F]altanserin separated from metabolites, but only clearly resolved the reduced alcohol [^{18}F]altanserinol. What we have called the "FBP" fraction actually consists of a mixture of metabolites that probably result from secondary metabolism of FBP. Detailed studies by the PET group at the University of Pittsburgh have shown that [^{18}F]FBP is converted to at least 1 other metabolite in rats and baboons (*20*). They reported that after administration of [^{18}F]FBP to baboons, radioactivity was uniformly distributed and was not displaced by the 5-HT$_{2A}$ antagonist SR 46349B (*21*). In this study, the fact that about 60% of [^{18}F]altanserin remained unmetabolized in plasma at early time points (37 and 67 min after injection) is consistent with previous kinetic studies (*17*). This value later stabilized at about 45% during the period of sustained equilibrium.

PET Measurements

The overall regional variability of uptake of [^{18}F]altanserin in this equilibrium study agreed with that of previous kinetic studies (*16–19*) as well as the known distribution of 5-HT$_{2A}$ receptors as seen in autoradiographic studies (*31–33*). After intravenous injection of a bolus plus constant infusion of [^{18}F]altanserin, radioactivity was high in all cerebral cortical regions and low in basal ganglia, thalamus, and cerebellum.

Ratios of total-to-nonspecific (cerebellar) binding between 6 and 10.5 h after injection were 1.97 ± 0.16 for the structure of highest uptake (anterior cingulate) and 1.75 ± 0.15 for whole cortex. The fact that these ratios were somewhat lower than previously reported for [^{18}F]altanserin kinetic studies (2.6) (*17*) is likely the result of: the greater age of our volunteers (mean, 32 versus 25 y); and the lower ratio of unmetabolized [^{18}F]altanserin inherent in a prolonged equilibrium compared with a kinetic paradigm (45% after 6 h of constant infusion versus 60% at 1 h after bolus injection). Our group is currently exploring the deuterium substitution of the 2′-hydrogen of altanserin ([^{18}F]deuteroaltanserin), yielding a metabolically more stable radiotracer with higher ratio of parent tracer to radiometabolites (*38*).

Distribution Volumes

The values of V_3 (as an estimate of the BP) calculated in this study (Table 2) are on the order of magnitude predicted from in vitro data. Pazos et al. (*32*) reported 5-HT$_2$ receptor densities of approximately 200–270 fmol/mg protein for those cortical regions analyzed in this study. Assuming approximately 10% protein in wet brain and 50% white matter in our PET ROIs, we would expect a B_{max} on the order of 10–13.5 nmol/L. The previously published K_i value (0.13 nmol/L) of altanserin for 5-HT$_2$ receptors (*13*) would thus predict BP values in the range of 77–104 for our cortical ROIs.

The outcome measure of choice for clinical studies remains to be determined. The stability in V_3 and V_3' once equilibrium is achieved suggests that a single long PET acquisition (e.g., 40 min) obtained at 6 h may provide a reasonable measure of 5-HT$_{2A}$ receptor density. V_3 (using individual measurements of f_1) has the theoretical advantage of directly estimating the BP but may lack reliability because of the difficulty of measuring f_1. The wide intersubject variability in f_1 points to the need to examine the intrasubject variability in f_1 as well. V_3' (or the proportionate measure of V_3 using a group mean f_1) rests on the questionable assumption of negligible intersubject variability in f_1, but may constitute a more reliable measure. Further test–retest studies are needed to establish the within-subject reliability of both outcome measures obtained from a single PET scan 6 h postinjection.

Assumptions of [^{18}F]Altanserin Equilibrium Modeling

The assumptions underlying the present model include: that cerebellum is relatively devoid of 5-HT$_{2A}$ receptors and thus lacks displaceable uptake; and that the nondisplaceable C_2 and C_{met} are uniformly distributed throughout the brain. Support for the second assumption is furnished by both rat autoradiographic studies (*39*) as well as human PET kinetic studies in which ketanserin pretreatment produced nonspecific binding of [^{18}F]altanserin and metabolites that was uniform in all brain regions (*17*).

With regard to the first assumption, the cerebellum has previously been used as a reference region for determination of 5-HT$_{2A}$ receptors in PET studies using [^{11}C]NMSP (*9,35*), [^{18}F]setoperone (*10,40*), and [^{18}F]altanserin (*16*). The choice of cerebellum as a reference region is based on the low levels of 5-HT$_{2A}$ receptors from postmortem studies (*31–33*). The aforementioned ketanserin pretreatment studies with [^{18}F]altanserin (*17*) supported the validity of estimating the nonspecific binding in cerebellum, revealing similar [^{18}F]altanserin kinetics in cerebellum during blocked and unblocked studies in the same individuals. Further competition studies should be conducted in nonhuman primates with competitors of well-defined specificity. The presence of a small component of specific binding in cerebellum may result in the underestimation of specific uptake in receptor-rich cortical regions using the proposed equilibrium model.

CONCLUSION

These results demonstrate the feasibility of equilibrium imaging with [^{18}F]altanserin and suggest a method to overcome difficulties associated with lipophilic radiolabeled metabolites. Further studies are needed to verify assumptions of the proposed model and to establish the reliability of outcome measures obtained from a single PET scan.

ACKNOWLEDGMENTS

The authors thank Dayton Rich and Quinn Ramsby for excellent technical assistance and Dr. Yolanda Zea-Ponce for helping with initial metabolite analysis method development. This research was supported by funds from the Department of Veterans Affairs (Schizophrenia Research Center and the VA Mental Illness Research, Education, and Clinical Center) and the Public Health Service (MH 30929).

REFERENCES

1. Arango V, Ernsberg P, Mazuk PM, et al. Autoradiographic demonstration of increased 5-HT2 and ß-adrenergic receptors in the brains of suicide victims. *Arch Gen Psychiatry.* 1990;47:1038–1047.
2. Stanley M, Mann JJ. Increased serotonin-2 binding sites in frontal cortex of suicide victims. *Lancet.* 1983;2:214–216.
3. Mita T, Hanada S, Nishino N, et al. Decreased serotonin S2 and increased dopamine D2 receptors in chronic schizophrenics. *Biol Psychiatry.* 1986;21:1407–1414.
4. Laruelle M, Abi-Dargham A, Casanova MF, Toti R, Weinberger DR, Kleinman JE. Selective abnormalities of prefrontal serotonergic receptors in schizophrenia: a postmortem study. *Arch Gen Psychiatry.* 1993;50:810–818.
5. Marcusson JO, Morgan DG, Winblad B, Finch CE. Serotonin-2 binding sites in human frontal cortex and hippocampus: selective loss of S-2A sites with age. *Brain Res.* 1984;311:51–56.
6. Reynolds GP, Arnold L, Rossor MN, Iversen LL, Mountjoy CQ, Roth M. Reduced binding of [^{3}H]ketanserin to cortical 5-HT$_2$ receptors in senile dementia of the Alzheimer type. *Neurosci Lett.* 1984;44:47–51.
7. Cross AJ, Crow TJ, Ferrier IN, Johnson JA. The selectivity of the reduction of serotonin S2 receptors changes in Alzheimer-type dementia. *Neurobiol Aging.* 1986;7:3–7.
8. Pike VP. Radioligands for PET studies of central 5-HT receptors and re-uptake sites—current status. *Nucl Med Biol.* 1995;22:1011–1018.
9. Wong DF, Wagner HN, Jr, Dannals RE, et al. Effects of age on dopamine and serotonin receptors measured by positron emission tomography in the living human brain. *Science.* 1984;226:1393–1396.
10. Blin J, Sette G, Fiorelli M, et al. A method for the in vivo investigation of the serotonergic 5-HT2 receptors in the human cerebral cortex using positron emission tomography and ^{18}F-labeled setoperone. *J Neurochem.* 1990;54:1744–1754.
11. Lemaire C, Cantineau R, Guillaume M, Plenevaux A, Christians L. Fluorine-18-altanserin: a radioligand for the study of serotonin receptors with PET: radiolabeling and *in vivo* biologic behavior in rats. *J Nucl Med.* 1991;32:2266–2272.
12. Lundkvist C, Halldin C, Ginovart N, et al. [^{11}C]MDL 100907, a radioligand for selective imaging of 5-HT$_{2A}$ receptors with positron emission tomography. *Life Sci.* 1996;58:187–192.
13. Leysen JE. Use of 5-HT receptor agonists and antagonists for the characterization of their respective receptor sites. In: Boulton AB, Baker GB, Jurio AV, eds. *Drugs as Tools in Neurotransmitter Research. Neuromethods.* Vol 12. Clifton, NJ: The Humana Press; 1989:299–349.
14. Mathis C, Choi Y, Simpson N, Mintun M. In vivo studies of 5-HT2 receptors in monkeys using F-18 altanserin [abstract]. *Soc Neurosci Abst.* 1994;20:1546.
15. Tan P-Z, Baldwin RM, van Dyck CH, et al. Characterization of radioactive metabolites of 5-HT2A receptor PET ligand [F-18]altanserin in human and rodent. *Nucl Med Biol.* 1999;26:601–608.
16. Biver F, Goldman S, Luxen A, et al. Multicompartmental study of fluorine-18 altanserin binding to brain 5HT$_2$ receptors in humans using positron emission tomography. *Eur J Nucl Med.* 1994;21:937–946.
17. Sadzot B, Lemaire C, Maquet P, et al. Serotonin 5HT$_2$ receptor imaging in the human brain using positron emission tomography and a new radioligand, [^{18}F]altanserin: results in young normal controls. *J Cereb Blood Flow Metab.* 1995;15:787–797.
18. Mintun M, Price J, Smith G, et al. Quantitative 5-HT2A receptor imaging in man using F-18 altanserin: a new model accounting for labeled metabolites [abstract]. *J Nucl Med.* 1996;37:109P.
19. Smith GS, Price JC, Mathis CA, et al. Test-retest variability ofserotonin 5-HT$_{2A}$ receptor binding measured with positron emission tomography and [^{18}F]altanserin in the human brain. *Synapse.* 1998;30:380–392.
20. Mason NS, Huang Y, Holt DP, Perevuznik JJ, Lopresti BJ, Mathis CA. Synthesis and characterization of [F-18]4-(4-fluorobenzoyl)piperidine, an [F-18]altanserin metabolite [abstract]. *J Nucl Med.* 1997;38:56P.
21. Mason NS, Huang Y, Holt DP, Perevuznik JJ, Lopresti BJ, Mathis CA. Synthesis of two radiolabeled metabolites of [^{18}F]altanserin: [^{18}F]3-[2-[4-(4-fluorophenyl-methanol)-1-piperidinyl]ethyl]-2,3-dihydro-2-thioxo-4-(1H)-quinazolinone and [^{18}F]4-(4-fluorobenzoyl)piperidine. *J Labelled Compds Radiopharm.* 1997;40:SI 161–162.
22. Frey KA, Ehrenkaufer LE, Beaucage S, Agranoff BW. Quantitative in vivo receptor binding I. Theory and application of the muscarinic cholinergic receptor. *J Neurosci.* 1985;5:421–428.
23. Carson RE, Channing MA, Blasberg RG, et al. Comparison of bolus and infusion methods for receptor quantitation: applications to [^{18}F]cyclofoxy and positron emission tomography. *J Cereb Blood Flow Metab.* 1993;13:24–42.
24. Tan P-Z, Baldwin RM, Soufer R, Garg PK, Charney DS, Innis RB. A complete remote-control system for reliable preparation of [^{18}F]altanserin, radioligand for imaging of 5-HT2A receptor in brain with positron emission tomography. *Appl Radiat Isot.* 1999;50:923–927.
25. Monclus M, Luxen A. A convenient synthesis of 4-nitrophenyl 4-piperidinyl ketone. *Organ Prep Pro Int.* 1992;24:692–694.
26. USP XXIII. Sterility tests <71>. In: *The United States Pharmacopeia.* 23rd rev ed. Rockville, MD: United States Pharmacopeial Convention; 1995:1686–1690.
27. Mullani NA, Gould KL, Hartz RK, et al. Design and performance of Posicam 6.5 BGO positron camera. *J Nucl Med.* 1990;31:610–616.
28. Matsui T, Hirano A. *An Atlas of the Human Brain for Computerized Tomography.* Tokyo, Japan: Igaku-Shoin, Ltd; 1978.
29. Gandelman MS, Baldwin RM, Zoghbi SS, Zea-Ponce Y, Innis RB. Evaluation of ultrafiltration for the free fraction determination of single photon emission computed tomography (SPECT) tracers: ß-CIT, IBF, and iomazenil. *J Pharm Sci.* 1994;83:1014–1019.
30. Mintun MA, Raichle ME, Kilbourn MR, Wooten GF, Welch MJ. A quantitative model for the *in vivo* assessment of drug binding sites with positron emission tomography. *Ann Neurol.* 1984;15:217–227.
31. Schotte A, Maloteaux JM, Laduron PM. Characterization and regional distribution of serotonin S$_2$-receptors in human brain. *Brain Res.* 1983;276:231–235.
32. Pazos A, Probst A, Palacios JM. Serotonin receptors in the human brain. IV. Autoradiographic mapping of serotonin-2 receptors. *Neuroscience.* 1987;21:123–139.
33. De Keyser J, Clayes A, De Backer JP, Ebinger G, Roels F, Vauquelin G. Autoradiographic localization of D1 and D2 receptors in the human brain. *Neurosci Lett.* 1988;91:142–147.
34. Laruelle M, Baldwin RM, Rattner Z, et al. SPECT quantification of [^{123}I]iomazenil binding to benzodiazepine receptors in nonhuman primates. I. Kinetic modeling of single bolus experiments. *J Cereb Blood Flow Metab.* 1994;14:439–452.
35. Wong D, Lever J, Hartig P, et al. Localization of serotonin 5-HT$_2$ receptors in living human brain by positron emission tomography using N^1-([^{11}C]-methyl)-2-Br-LSD. *Synapse.* 1987;1:393–398.
36. Rosier A, Dupont P, Peuskens J, et al. Visualisation of loss of 5-HT$_{2A}$ receptors with age in healthy volunteers using [^{18}F]altanserin and positron emission tomographic imaging. *Psychiatry Res Neuroimaging.* 1996;68:11–22.
37. Meltzer CC, Smith G, Price JC, et al. Reduced binding of [^{18}F]altanserin to serotonin type 2A receptors in aging: persistence of effect after partial volume correction. *Brain Res.* 1998;813:167–171.
38. Tan P-Z, Baldwin RM, Fu T, Charney DS, Innis RB. Rapid synthesis of F-18 and H-2 dual-labeled altanserin, a metabolically resistant PET ligand for 5-HT2A receptors. *J Labelled Compds Radiopharm.* 1999;42:457–467.
39. Biver F, Goldman S, Monclus M, Luxen A, Lotstra F, Mendlewicz J. Autoradiographic study of [^{18}F]altanserin in the rat: a potential radiotracer for 5HT$_2$ receptor study with PET. *Clin Neuropharmacol.* 1992;15(suppl 1):202.
40. Blin J, Baron J, Dubois B, et al. Loss of brain 5-HT2 receptors in Alzheimer's disease. *Brain.* 1993;116:497–510.